

# New insights into the solution equilibrium of molybdenum(vi)–hydroxamate systems: $^1\text{H}$ and $^{17}\text{O}$ NMR spectroscopic study of Mo(vi)–desferrioxamine B and Mo(vi)–monohydroxamic acid systems

Etelka Farkas,\* Hajnalka Csóka and Imre Tóth

Department of Inorganic and Analytical Chemistry, University of Debrecen, H-4010 Hungary.

E-mail: efarkas@delfin.klte.hu

Received 13th January 2003, Accepted 18th February 2003

First published as an Advance Article on the web 6th March 2003

To complement our previous pH-potentiometric and spectrophotometric investigations, in the present work  $^{17}\text{O}$  NMR studies on Mo(vi)–desferrioxamine B (DFB) and Mo(vi)–acetohydroxamic acid (Aha) systems, and  $^1\text{H}$  NMR on Mo(vi)–Aha, Mo(vi)–benzohydroxamic acid (Bha) and *N*-methylacetohydroxamic acid (MeAha) have been performed. Complete equilibrium models for all the studied systems are presented in this paper. Formation of a hydrogen bond could be suggested between the hydroxamate-NH of the coordinated primary monohydroxamic acids and oxo ligands of molybdenum under acidic conditions and, at *ca.* neutral pH, deprotonation of that NH was found. This is the first time that this process in a Mo(vi)–hydroxamic acid system has been detected. The hydroximato chelate formed in this manner is unusually stable, and able to compete with hydrolytic processes up to basic pH, which results in the surprising fact that the interaction between Mo(vi) and the small primary molecules, Aha and Bha exists up to much higher pH than between Mo(vi) and the known powerful tris-chelator natural compound, DFB.

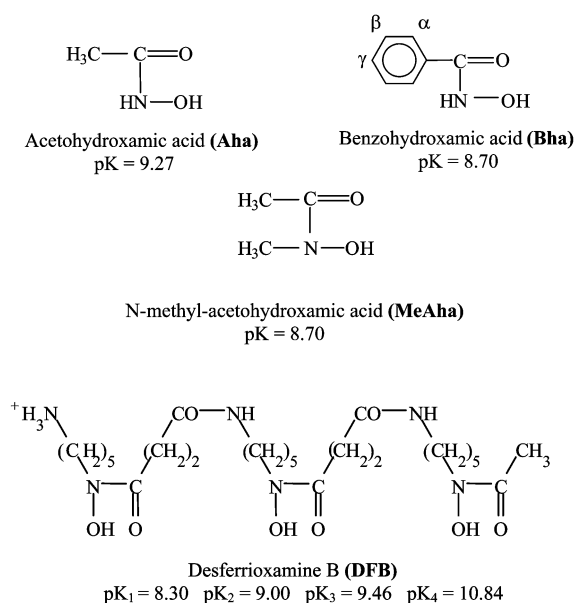
## Introduction

The essential role of siderophores in the iron uptake of microbes is well known.<sup>1,2</sup> Recent investigations supported the role of siderophores also in molybdenum uptake in  $\text{N}_2$ -fixing bacteria.<sup>3,4</sup> It was found that the amount of siderophore released by these microbes is influenced by the concentration of molybdate in the growth medium.<sup>4</sup> In spite of their possible biological importance, molybdenum–hydroxamate based siderophore systems have not been studied extensively.<sup>5–11</sup> Very strong interaction between desferrioxamine B (DFB =  $\text{H}_4\text{L}^+$ ) and Mo(vi) in acidic solution was shown by our previous pH-potentiometric and UV–VIS investigations.<sup>7</sup> Equimolar amount of DFB hinders the formation of polyoxomolybdates completely and a metal complex  $[\text{MoO}_2(\text{H}_2\text{L})]^+$  is formed in which DFB is coordinated to a dioxomolybdenum core ( $\text{MoO}_2^{2+}$ ) *via* its two hydroxamate chelates while its non-coordinated hydroxamic plus terminal amino groups are still protonated. This complex hydrolyses in cooperative processes above pH 5 and only the molybdate and the free ligand were found above pH *ca.* 7.5.<sup>7</sup>

Equilibrium systems involving Mo(vi) and different monohydroxamic acids (hereafter their general abbreviation is HL) are more complicated than the Mo(vi)–DFB system.<sup>8–11</sup> Namely, the bis-chelated complexes,  $[\text{MoO}_2\text{L}_2]$  formed in the molybdenum(vi)–monohydroxamic acid systems are somewhat less stable, and the two hydroxamate chelates are displaced in consecutive hydrolytic processes which results in the formation of a mono-chelated type complex in measurable concentration under slightly acidic and neutral conditions. Many ligands containing three donors form stable octahedral mono-complexes with an  $\text{MoO}_3$  core,<sup>12</sup> but a hydroxamate function contains only two donors. This means that, at least theoretically, two different types of mono-chelated hydroxamate complex,  $[\text{MoO}_3\text{L}(\text{H}_2\text{O})]^-$  and  $[\text{MoO}_2\text{L}(\text{OH})_2]^-$ , can be formed but neither pH-potentiometry, nor spectrophotometry can differentiate between them. Consequently, the question as to whether one or the other, or both of them are formed remained open in our previous work.<sup>7</sup> Fortunately,  $^{17}\text{O}$  NMR chemical shifts related to the number and types of oxo ligands in the molecules,<sup>13,14</sup> and perhaps  $^1\text{H}$  NMR methods might provide an answer to the

above question and offer new insight into the solution equilibrium of Mo(vi)–hydroxamate systems.

Now we have complemented our previous pH-potentiometric and UV–VIS spectrophotometric work, further studying the interaction between Mo(vi) and hydroxamates.  $^{17}\text{O}$  NMR measurements were performed on the Mo(vi)–DFB and Mo(vi)–Aha systems and  $^1\text{H}$  NMR investigations were made on the Mo(vi)–Aha, Mo(vi)–Bha and Mo(vi)–MeAha systems. The formulae of the ligands together with the corresponding dissociation constants are shown in Scheme 1.



Scheme 1

## Experimental

### Chemicals

The molybdenum(vi) stock solution was prepared from  $\text{Na}_2\text{MoO}_4$  (Reanal). Acetohydroxamic acid and benzohydroxamic

acid were SIGMA products, *N*-methylacetoxyhydroxamic acid was prepared by standard procedures from the corresponding carboxylic esters and hydroxylamine,<sup>15</sup> and DFB was produced by CIBA-GEIGY. The concentration of the metal ion stock solution was checked gravimetrically *via* precipitation of the quinolin-8-olate. The concentration of the ligand stock solutions was determined by pH-metry by the use of Gran's method.<sup>16</sup> Literature data ( $\log \beta$ ) for the molybdenum(VI) hydrolytic species were used during the calculations:  $[\text{HMoO}_4]^-$  4.03;  $[\text{H}_2\text{MoO}_4]$  6.70;  $[\text{H}_8(\text{MoO}_4)_7]^{6-}$  53.18;  $[\text{H}_9(\text{MoO}_4)_7]^{5-}$  58.10;  $[\text{H}_{10}(\text{MoO}_4)_7]^{4-}$  62.11;  $[\text{H}_{11}(\text{MoO}_4)_7]^{3-}$  64.54.<sup>7</sup> All the measurements were made at 25 °C and at 0.2 M KCl.

Carbonate-free KOH solutions of known concentrations (*ca.* 0.2 M during the pH-metric measurements and *ca.* 5 M to adjust the pH during the <sup>17</sup>O NMR measurements) were used as titrant. HCl stock solutions were prepared from 37% HCl (m/m) (both the acid and base were Merck products) and their concentrations were determined by pH-metric titrations.

### Potentiometric <sup>17</sup>O and <sup>1</sup>H NMR studies

A Radiometer pHM 84 instrument equipped with Metrohm combined electrode (type 6.0234.110) and Metrohm 715 Dosimat burette was used to measure the pH and pD values. The pD values were converted to pH values as usual:

$$\text{pD} = \text{pH meter reading} + 0.4.$$

The electrode system was calibrated according to Irving *et al.*,<sup>17</sup> and the pH-metric readings could therefore be converted into hydrogen ion concentration. The water ionization constant,  $\text{p}K_w$ , is  $13.76 \pm 0.01$  under the conditions employed. The pH-metric titrations were performed in the pH range 2.0–10.5. The initial volume of the samples was 10.00 cm<sup>3</sup>. The PSEQUAD computer program<sup>18</sup> was used to fit the experimental data. Because numerous species are co-present in a Mo(VI)-containing system but the free metal ion does not exist in aqueous solution, as usual,  $\text{MoO}_4^{2-}$  was chosen as the component M in the calculations. Standard deviations are always given in parentheses for the stability constants calculated in the present work.

<sup>17</sup>O NMR measurements were performed for the Mo(VI)–Aha and Mo(VI)–DFB systems at 1 : 3 and 1 : 1.2 metal to ligand ratios, and at  $c_{\text{ligand}} = 0.15$  and 0.03 M, respectively. The solvent was 90% H<sub>2</sub>O–10% D<sub>2</sub>O enriched for <sup>17</sup>O. Enrichment of the molybdate oxygen atoms to 3% was done by addition of H<sub>2</sub><sup>17</sup>O (12%, Cambridge Isotope Laboratories) to the samples. The enrichment included the M=O oxygens, while the oxygens of the ligands were not involved in the <sup>17</sup>O isotope enrichment, being inert for oxygen exchange. Spectra were registered on Bruker DRX 500 NMR equipment at 67.8 MHz. Spectral widths of 1200 ppm (81.4 kHz) were used, and data for the FID were accumulated in 8k blocks. A 40° pulse angle and 100 ms relaxation delays were used. The spectra were integrated after baseline correction by using WINNMR software. Chemical shifts refer to the signal of tap water,  $\delta = 0$  ppm.

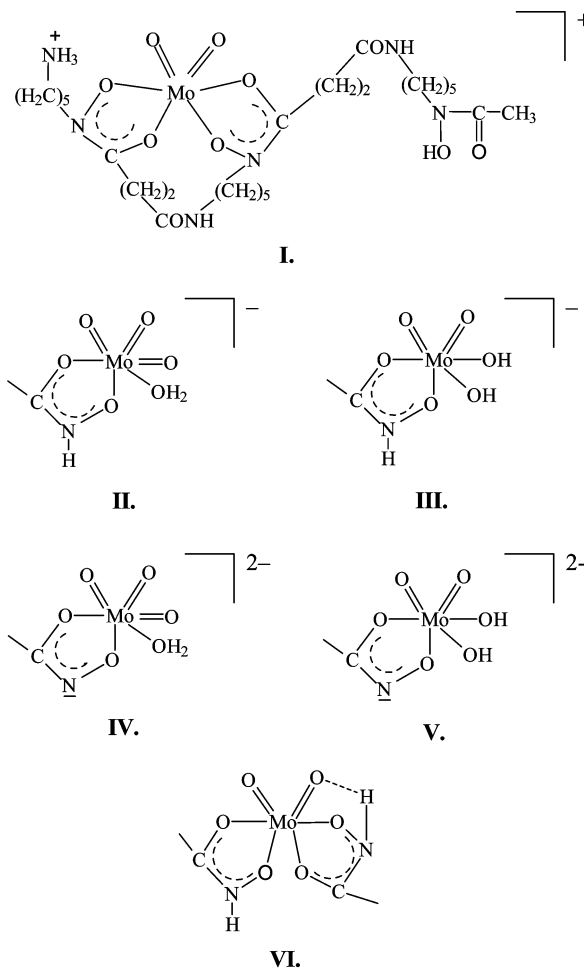
<sup>1</sup>H NMR measurements were made on Bruker AM 360 by using D<sub>2</sub>O as solvent using DSS (sodium 4,4'-dimethyl-4-silapentane-1-sulfonate) as standard at the following conditions: Metal to ligand ratio was 1 : 3 in all samples and the analytical concentrations were as follows:  $c_{\text{Bha}} = c_{\text{MeAha}} = ca. 0.015$  M,  $c_{\text{Aha}} = 0.15$  M. 15–25 spectra were recorded in the following pD-ranges: *ca.* 2–11.5 for the Mo(VI)–Aha, *ca.* 2–8 for the Mo(VI)–MeAha and *ca.* 5–11 for the Mo(VI)–Bha systems.

## Results and discussion

### <sup>17</sup>O NMR results for the Mo(VI)–DFB system

The pH-potentiometric equilibrium model for the Mo(VI)–DFB system is very simple.<sup>7</sup> All titration curves (more than 250 experimental data) could be fitted (fitting parameter was

$4 \times 10^{-3} \text{ cm}^3$ ) with the model involving the proton complexes of DFB (Scheme 1), hydroxo species of molybdenum(VI) (see Experimental section) and the metal complex,  $[\text{MoO}_2(\text{H}_2\text{L})]^+$  (schematic view of one of the possible bonding modes is shown by I in Scheme 2).



Scheme 2

The overall constant  $\log \beta$ , obtained for the equilibrium (1) is 53.54.



$$\beta_{[\text{MoO}_2(\text{H}_2\text{L})]^+} = \frac{[\text{MoO}_2(\text{H}_2\text{L})]^+}{[\text{MoO}_4^{2-}][\text{L}^{3-}][\text{H}^+]^6}$$

The corresponding concentration distribution curves are presented in Fig. 1(a).

According to Fig. 1(a), the metal complex,  $[\text{MoO}_2(\text{H}_2\text{L})]^+$  existing exclusively below pH 5 decomposes “in a single step” by pH *ca.* 7.5. Also, the UV–VIS spectra show the characteristic band of  $[\text{MoO}_2(\text{H}_2\text{L})]^+$  ( $\lambda_{\text{max}}$  and  $\epsilon$  values are 290 nm and *ca.*  $2.9 \times 10^3 \text{ M}^{-1} \text{ cm}^{-1}$ , respectively) below pH 5 exclusively; the intensity of this band starts to decrease at pH 5 and disappears at *ca.* pH 7.5–8.

Owing to the high basicity of the hydroxamate and amino groups of DFB, the completely protonated ligand is formed in the decomposition reaction (2).



In order to obtain further evidence for the equilibrium model of the Mo(VI)–DFB system, <sup>17</sup>O NMR investigation under the conditions given in the Experimental section have

**Table 1** Comparison of number of oxo ligands, chemical shifts of  $^{17}\text{O}$  signals, Mo–O distances, and expected  $\pi$ -bond orders for the various molybdenum cores<sup>a</sup>

|                       | $\text{MoO}_4^{2-}$ | <i>cis</i> - $\text{MoO}_3$ | <i>cis</i> - $\text{MoO}_2^{2+}$ |
|-----------------------|---------------------|-----------------------------|----------------------------------|
| Number of oxo ligands | 4                   | 3                           | 2                                |
| $\pi$ -Bond order     | 0.75                | 1                           | 1.5                              |
| Bond length/pm        | 176                 | 173                         | 170                              |
| Chemical shift/ppm    | 532                 | ~700                        | ~900                             |

<sup>a</sup> The values are taken from ref. 13.

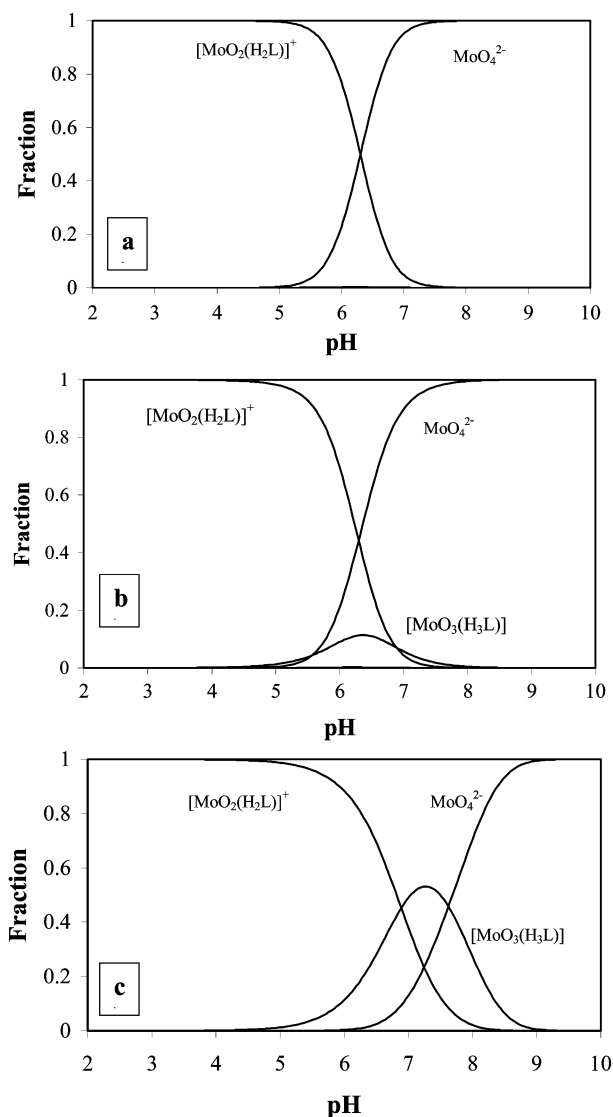


**Fig. 1** Concentration distribution curves calculated for the Mo(vi)-DFB system by the use of the pH-metric model<sup>7</sup> at  $c_{\text{DFB}} = 0.003 \text{ M}$ ,  $c_{\text{Mo(vi)}} = 0.0025 \text{ M}$  (a);  $^{17}\text{O}$  NMR model at  $c_{\text{DFB}} = 0.003 \text{ M}$ ,  $c_{\text{Mo(vi)}} = 0.0025 \text{ M}$  (b);  $^{17}\text{O}$  NMR model at  $c_{\text{DFB}} = 0.03 \text{ M}$ ,  $c_{\text{Mo(vi)}} = 0.0025 \text{ M}$  (c).

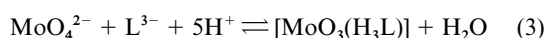
been performed. Selected NMR spectra are shown in Fig. 2 and the intensities of the signals as a function of pH are presented in the inset in Fig. 2.

As Fig. 2 shows, only one signal at *ca.* 900 ppm appears below pH 5. A comparison of this chemical shift with those given in Table 1 supports unambiguously that the peak belongs to a  $\text{MoO}_2^{2+}$  core-containing complex.

Substantial broadening of the signal could be attributed to intramolecular exchange processes between the possible bonding isomers (coordination of different two of the three hydroxamates) or between different optical and geometrical isomers. The inset in Fig. 2 indicates that the dioxomolybdenum-

containing species exists practically at 100% below pH 5. At pH 5.25, however, a new signal at *ca.* 680 ppm appears, which strongly suggests the appearance of some species containing a trioxomolybdenum core (*cf.* Table 1). The intensity of this signal increases up to *ca.* pH 7, decreases when the pH is increased further, and finally disappears by *ca.* pH 8.5. The characteristic  $^{17}\text{O}$  signal of  $\text{MoO}_4^{2-}$  starts to develop at 530 ppm at *ca.* pH 6, and exclusively exists above pH 8.5. The intermolecular exchange between the  $[\text{MoO}_2(\text{H}_2\text{L})]^+$  and  $[\text{MoO}_3(\text{H}_3\text{L})]$  can be neglected, because any broadening of the signal of the latter complex can not be observed.

Thus, the NMR results show clearly that a mono-chelated species containing a trioxomolybdenum core also appears in a narrow pH-range in the system. By the use of this new model the pH-metric experimental data were fitted again and the overall stability constants ( $\log \beta$ ) for the complexes  $[\text{MoO}_2(\text{H}_2\text{L})]^+$  and  $[\text{MoO}_3(\text{H}_3\text{L})]$  were calculated. They are 53.56(3) and 46.67(6) for the overall processes (1) and (3), respectively (fitting parameter  $3 \times 10^{-3} \text{ cm}^3$ ).

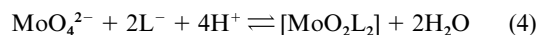


$$\beta_{[\text{MoO}_3(\text{H}_3\text{L})]} = \frac{[\text{MoO}_3(\text{H}_3\text{L})]}{[\text{MoO}_4^{2-}][\text{L}^{3-}][\text{H}^+]^5}$$

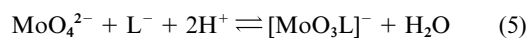
Why was the complex  $[\text{MoO}_3(\text{H}_3\text{L})]$  previously not found by pH-metry? Most probably, because it was formed in a very narrow pH-range and in a very low concentration under the conditions applied. It is important to appreciate that different analytical concentrations were used for the pH-metric and NMR methods. In the pH-metric measurements  $c_{\text{DFB}}$  was varied in the range of 0.001–0.003 M and the metal to ligand ratios were 1 : 1, 1 : 2 and 1 : 3.  $^{17}\text{O}$  NMR measurements were, however, performed at much higher analytical concentrations, *i.e.*  $c_{\text{DFB}} = 0.03 \text{ M}$  and  $c_{\text{Mo(vi)}} = 0.025 \text{ M}$ . The effect of this concentration difference on the concentration distribution curves is demonstrated in Fig. 1(b) and (c). The former relates to the conditions used during the pH-metric measurements, the latter to the conditions of  $^{17}\text{O}$  NMR measurements. Fig. 1(b) and (c) show that under the condition of  $^{17}\text{O}$  NMR measurements the maximum concentration of the species  $[\text{MoO}_3(\text{H}_3\text{L})]$  is *ca.* 50% (which at the same time agrees quite well with the fraction calculated by the intensities of the signals and shown in the inset in Fig. 2) but it is less than 10% under the pH-potentiometric conditions. This should be the reason why the pH-titration curves could be well fitted without involving  $[\text{MoO}_3(\text{H}_3\text{L})]$  in the equilibrium model.

#### $^{17}\text{O}$ NMR results for the Mo(vi)-Aha system

According to the pH-metric and spectrophotometric results<sup>7</sup>  $[\text{MoO}_2\text{L}_2]$  and  $[\text{MoO}_3\text{L}]^-$  are formed in the Mo(vi)-Aha system, and the interaction between the metal ion and the ligand exists only below pH *ca.* 8.5. The overall stability constants ( $\log \beta$ ) reported for the processes (4) and (5) are 32.46 and 17.16, respectively.



$$\beta_{[\text{MoO}_2\text{L}_2]} = \frac{[\text{MoO}_2\text{L}_2]}{[\text{MoO}_4^{2-}][\text{L}^-]^2[\text{H}^+]^4}$$



$$\beta_{[\text{MoO}_3\text{L}]^-} = \frac{[\text{MoO}_3\text{L}]^-}{[\text{MoO}_4^{2-}][\text{L}^-][\text{H}^+]^2}$$

There is no doubt that two hydroxamates coordinate to the dioxomolybdenum core in the species  $[\text{MoO}_2\text{L}_2]$ , but what is the

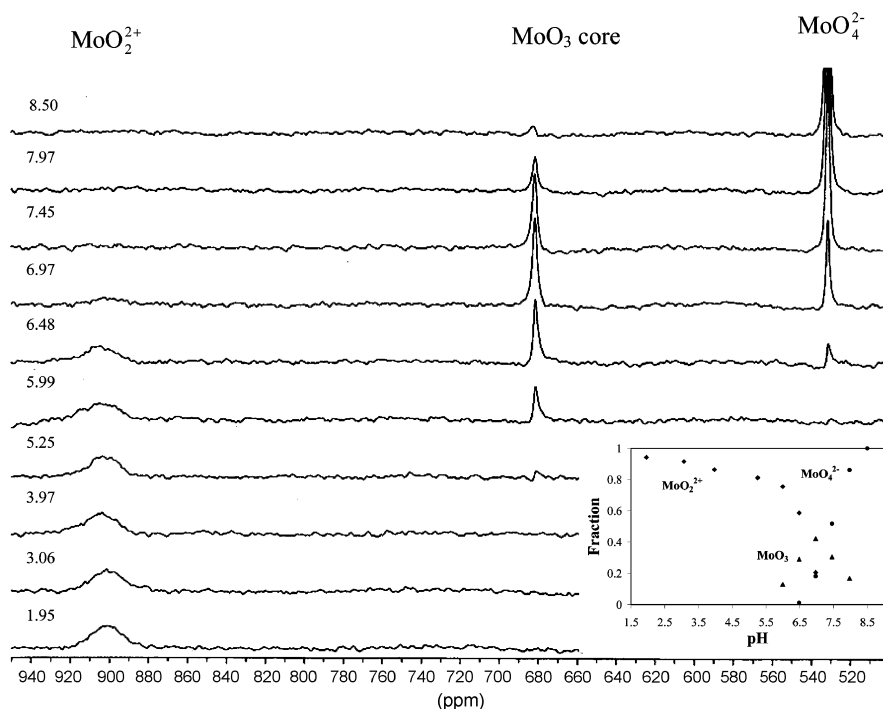


Fig. 2  $^{17}\text{O}$  NMR spectra of the Mo(vi)-DFB system at pH values shown on the spectra; inset: pH-dependence of the relative intensities of the various signals:  $c_{\text{DFB}} = 0.03 \text{ M}$ ,  $c_{\text{Mo(vi)}} = 0.025 \text{ M}$ .

bonding mode in the monochelated complex,  $[\text{MoO}_3\text{L}]^-$ ? The possible two complexes, (II) and (III), could not be differentiated by the methods used in the previous study. One of the main aims of the present NMR study was to solve this problem.

$^{17}\text{O}$  NMR spectra of Mo(vi)-Aha were registered between pH *ca.* 2.0–11.7 at metal to ligand ratio 1 : 3 (Fig. 3). The signals were assigned with the use of the characteristic chemical shifts shown in Table 1.

Surprisingly, the spectra in Fig. 3 indicate two well-defined deprotonation processes of the complexes containing  $\text{MoO}_2^{2+}$  and one of the complex containing the  $\text{MoO}_3$  core. This means that three different types of  $\text{MoO}_2^{2+}$ -containing and two  $\text{MoO}_3$ -containing species are formed in this system. Moreover, the  $\text{MoO}_2^{2+}$  core is extremely stable and exists up to pH 10–10.5. If the chemical shift *vs.* pH curves shown in the inset in Fig. 3 are fitted by the computer program PSEQUAD, the following dissociation constants (*pK*) are obtained:  $pK_1 = 4.45(1)$ ,  $pK_2 = 6.74(1)$  for the  $\text{MoO}_2^{2+}$ -containing species and  $pK = 7.73(1)$  for the  $\text{MoO}_3$ -containing one.

Relative intensities of the  $^{17}\text{O}$  signals were used to quantify the amount of species involving the different cores ( $\text{MoO}_2^{2+}$ ,  $\text{MoO}_3$  and  $\text{MoO}_4^{2-}$ ). Fig. 4 shows these values (individual points) together with the pH-metrically determined concentration distribution curves (solid lines).

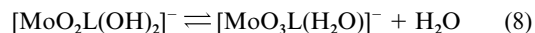
The conclusions that can be drawn from the NMR results are the following:

(i) Only the characteristic signal of  $\text{MoO}_2^{2+}$  appears in Fig. 3 at *ca.* pH 2 which suggests the exclusive formation of  $[\text{MoO}_2\text{L}_2]$ . On increasing the pH above 2, the chemical shift of that signal tends to decrease and the  $pK_1 = 4.45$  (see above) can be attributed to the process occurring in this pH-range. On the other hand, the signal of  $\text{MoO}_3$  can not be observed below *ca.* pH 4. These findings indicate the formation of a new  $\text{MoO}_2^{2+}$ -containing complex in this pH range. This is most probably the species  $[\text{MoO}_2\text{L}(\text{OH})_2]^-$  (III) formed in eqn. (6) (the non-coordinated Aha is in its protonated form).



(ii) The very broad NMR signal of  $\text{MoO}_3$  oxygens is clearly observable at *ca.* 688 ppm at *ca.* pH 4 (Fig. 3) and at the same

time the intensity of the signal belonging to the oxo ligands of  $\text{MoO}_2^{2+}$  starts to decrease somewhat. These two findings strongly suggest the appearance of  $[\text{MoO}_3\text{L}(\text{H}_2\text{O})]^-$  (II) in the equilibrium (7) or (8) or in both of them.



Interesting changes in the line-width of  $\text{MoO}_3$  signal as a function of pH show remarkable intramolecular exchange processes in  $[\text{MoO}_3\text{L}(\text{H}_2\text{O})]^-$ . The large broadening of that signal can not be attributed to a two-site intermolecular exchange with  $\text{MoO}_2^{2+}$ -containing species, the signal of which is actually less broadened. The temperature dependence of the spectrum at pH = 4.81 showed that the  $\text{MoO}_2$  signal became slightly broadened at 273 K, as is a normal behaviour for a  $^{17}\text{O}$  signal in a more viscous sample. The signal of the  $\text{MoO}_3$  core, however, became substantially sharpened. This kind of temperature dependence of the line-width is typical for a signal being in slow exchange, because the exchange reaction is slower at lower temperature. The exchange site should be the water, but the effect on the water signal is hardly visible because of its large population. To study this problem in detail, however, is beyond the scope of this work.

(iii) According to the pH-metric model, the concentration of  $[\text{MoO}_3\text{L}(\text{H}_2\text{O})]^-$  starts to decrease and  $\text{MoO}_4^{2-}$  appears at *ca.* pH 6, and by pH 9 the latter species exists exclusively (see continuous lines in Fig. 4). Although the intensity of the  $^{17}\text{O}$  signal of  $\text{MoO}_3$  starts to decrease at *ca.* pH 5.5 the simple pH-metric model is not supported by the NMR results. Namely, the formation of a new  $\text{MoO}_3$ -containing species is indicated by the shift of the less and less intense  $^{17}\text{O}$  signal ( $pK = 7.73$ ). Moreover, the intensity of the signal of  $\text{MoO}_2^{2+}$  does not decrease, but on the contrary, it starts to increase a little bit again at *ca.* pH 6. Parallel with that, the shift of this signal shows a "second deprotonation process" (corresponding  $pK_2 = 6.74$ ) and the formation of a third type of complex containing  $\text{MoO}_2^{2+}$ . The signal of  $\text{MoO}_4^{2-}$  becomes observable at *ca.* pH 5.7, but exclusively exists only above 10.

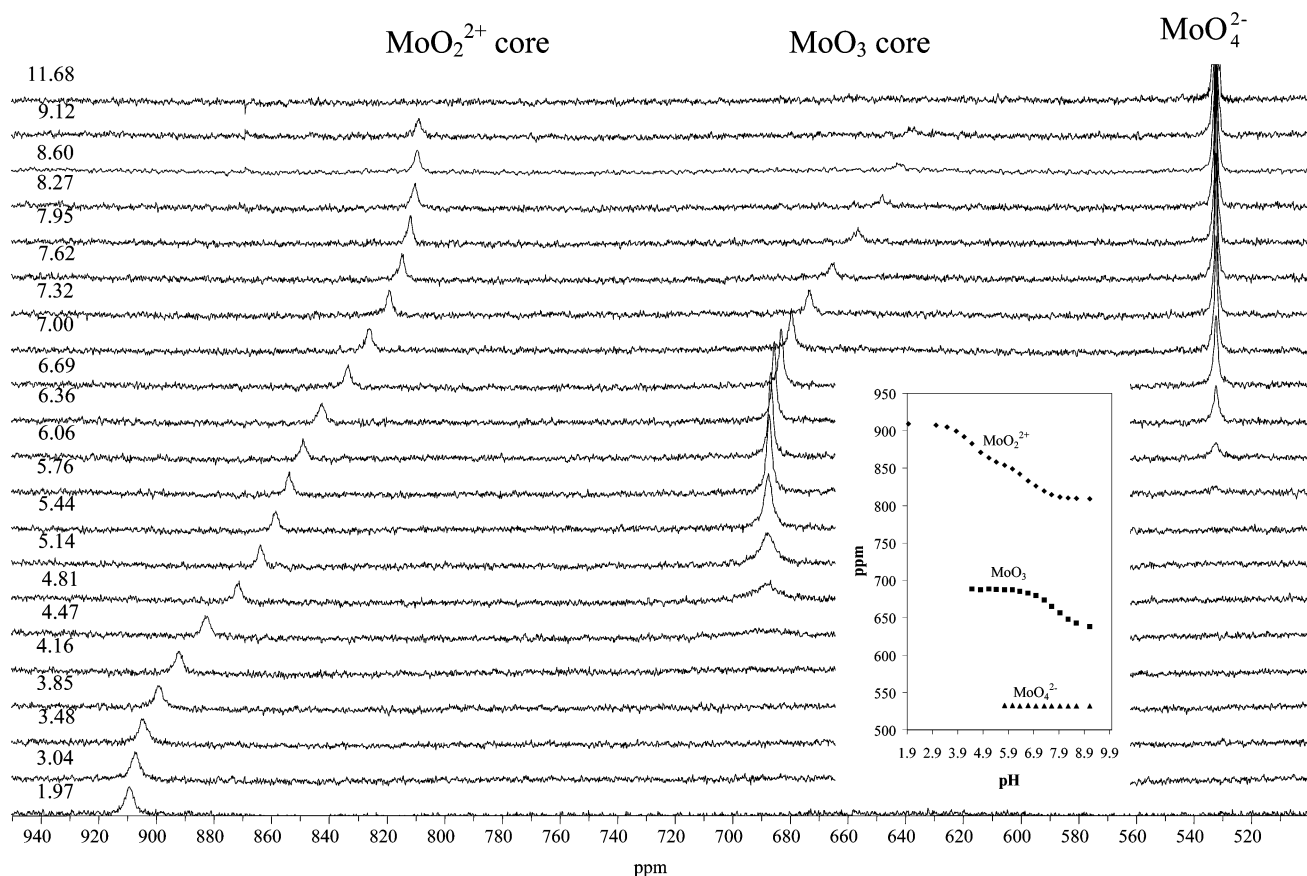


Fig. 3  $^{17}\text{O}$  NMR spectra of Mo(VI)-Aha recorded at metal to ligand ratio 1 : 3, at pH values shown on the spectra:  $c_{\text{Aha}} = 0.15 \text{ M}$ ,  $c_{\text{Mo(vi)}} = 0.05 \text{ M}$ .

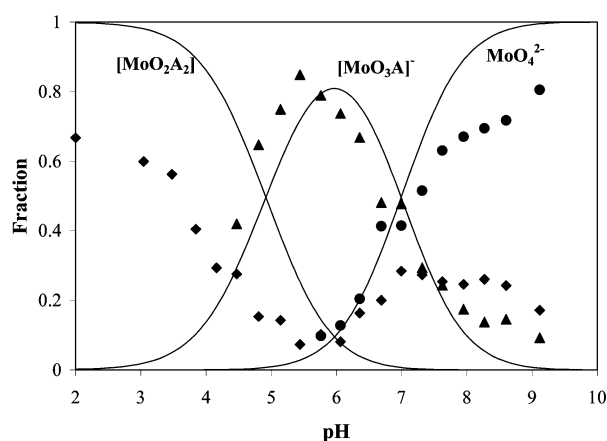
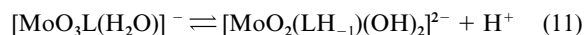
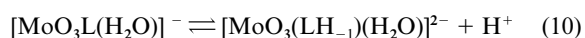
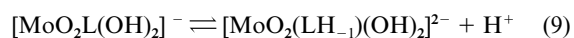


Fig. 4 Relative intensities (fractions) of the  $^{17}\text{O}$  NMR signals for the  $\text{MoO}_2^{2+}$  ( $\blacklozenge$ ),  $\text{MoO}_3$  ( $\blacktriangle$ ) containing complexes,  $\text{MoO}_4^{2-}$  ( $\bullet$ ) and the pH-metrically determined concentration distribution curves (continuous lines) of Mo(VI)-Aha complexes:  $c_{\text{Aha}} = 0.15 \text{ M}$ ,  $c_{\text{Mo(vi)}} = 0.05 \text{ M}$ .

The most likely explanation of these unexpected results is that the deprotonation of the NH in the coordinated hydroxamate (as was previously found in the Cu(II)-Aha complex at high pH<sup>19</sup>) occurs above pH *ca.* 6–7, which results in the formation of the significantly more stable hydroximato chelate (structures IV, V). The formation of (IV) and (V) may be responsible for the unexpectedly strong interaction obtained between Aha and molybdenum under basic condition. The most likely deprotonation processes resulting in the formation of the hydroximato complexes are shown in eqns (9)–(11).



The formation of the two hydroximato complexes involves the same pH-effect as the formation of  $\text{MoO}_4^{2-}$  in eqns. (12) and (13). Moreover, their decomposition to free ligand (HL) and  $\text{MoO}_4^{2-}$  does not involve a pH-effect. This should be the reason why the pH-metry was not able to detect the formation of these hydroximato species.



If the N–H bond is polarised in the Mo(VI)-Aha hydroxamate complexes, a strong intramolecular hydrogen bond between the NH proton and an oxo ligand (*e.g.* structure VI) might occur already at acidic conditions. The formation of such an intramolecular hydrogen bond can cause some “apparent” decrease of the  $\text{MoO}_2^{2+}$  core species, which might account, at least in some part, for the unexpectedly low Mo fraction in the pH range *ca.* 2–4. Perhaps, another part of the “missing fraction” is in  $\text{MoO}_3$ -containing species having a very broad, unobservable  $^{17}\text{O}$  signal (see molar fractions in Fig. 4).

By the use of the new equilibrium model and the *pK* values relating the deprotonation processes of the various molybdenum core-containing complexes, plus the fractions calculated from the relative intensities of the signals pH above 5, the stability constants the complexes and their concentration distribution curves were calculated (Fig. 5).

Comparison of Figs. 4 and 5 shows that the concentration distribution curves shown in Fig. 5 fit very well with the Mo fractions calculated from the NMR spectra (see Fig. 4) except pH below 4 in which region some part of the intensity of the  $^{17}\text{O}$  NMR signal is missing. The possible cause of this “anomaly” is explained above by the formation of a hydrogen bond between the NH proton and an oxo ligand.

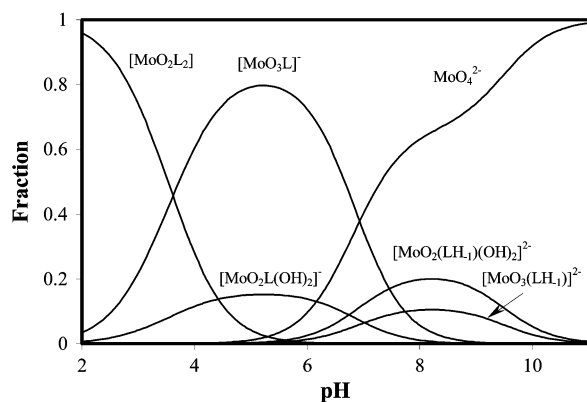


**Fig. 5** Concentration distribution curves for the complexes formed in the Mo(vi)-Aha system calculated by the use of the  $^{17}\text{O}$  NMR spectra  $\log\beta$  values:  $[\text{MoO}_2\text{L}_2]$ : 31.13,  $[\text{MoO}_3\text{L}]^-$ : 17.13,  $[\text{MoO}_2\text{L}(\text{OH})_2]^-$ : 16.41,  $[\text{MoO}_3(\text{LH}_{-1})]^{2-}$ : 9.39,  $[\text{MoO}_2(\text{LH}_{-1})(\text{OH})_2]^{2-}$ : 9.67;  $c_{\text{Aha}} = 0.15$  M,  $c_{\text{Mo(vi)}} = 0.05$  M.

If our assumption regarding the formation of hydroxamate complexes is correct, the same processes can occur with other primary hydroxamic acids such as Bha but not with secondary hydroxamic acids (like with DFB, MeAha). Unfortunately, the selected monohydroxamic acids (Bha, MeAha) and especially their molybdenum complexes had too low solubility to perform  $^{17}\text{O}$  NMR studies with them.

#### $^1\text{H}$ NMR results for the Mo(vi)-Aha, Mo(vi)-Bha and Mo(vi)-MeAha systems

In order to get further support to the equilibrium model of the Mo(vi)-monohydroxamate interaction, two additional systems, Mo(vi)-Bha and Mo(vi)-MeAha were studied. A pH-potentiometric and spectrophotometric investigations of the latter two systems were previously made.<sup>11</sup> The results obtained were very similar to those of Mo(vi)-Aha and the stability constants ( $\log\beta$ ) determined for the complexes  $[\text{MoO}_2\text{L}_2]$  and  $[\text{MoO}_3\text{L}(\text{H}_2\text{O})]^-$  of Bha and MeAha (for eqns. (4) and (5)) are 32.35, 31.90 and 16.89, 16.89, respectively.

$^1\text{H}$  NMR investigations on the H-Aha, Mo(vi)-Aha, H-Bha, Mo(vi)-Bha, H-MeAha and Mo(vi)-MeAha systems were performed. For the ligand spectra the H-Aha and H-MeAha systems showed simple behavior (not shown).  $^1\text{H}$  NMR spectra for the H-Aha system involve practically only one singlet appearing at 1.915 ppm in the pD-range 2.0–7.6 and above this pD the deprotonation of the ligand results in the decrease of the chemical shift down to 1.791 ppm at pD = 11.8. In the pD-range 2–8 two singlets at 2.09 and 3.20 ppm for the H-MeAha system appear which belong to the methyl protons next to the C and N atoms, respectively. Since even in very dilute solutions, precipitation occurred in the acidic region in the Mo(vi)-Bha samples, spectra could only be recorded in the pD-range ca. 5–11. For this reason the ligand spectra were recorded only in the same pD range.

Some of the spectra recorded for the Mo(vi)-Aha, H-Bha and Mo(vi)-Bha systems are shown in Fig. 6 and in Fig. 7(a) and (b), respectively.

It can be seen in Fig. 6 that in addition to the free Aha signal † another one showing two deprotonation steps exists almost in the whole studied pD range and disappears only above pD 10. At pD = 2.01 the relative intensity of the two observed signals is exactly 2 : 1. Because the metal to ligand ratio in the sample was 1 : 3, this finding shows that two thirds of the ligand exists in the complex and one third of it is free at this pD. Interesting

† The very weak peak appearing at 2.10 ppm in the pD-range 2–8 and shifting down to 1.97 ppm by pD = 11.77 belongs most probably to an isomeric form of Aha which does not take part in any complex formation. (The peak appears also in the free ligand spectra.)

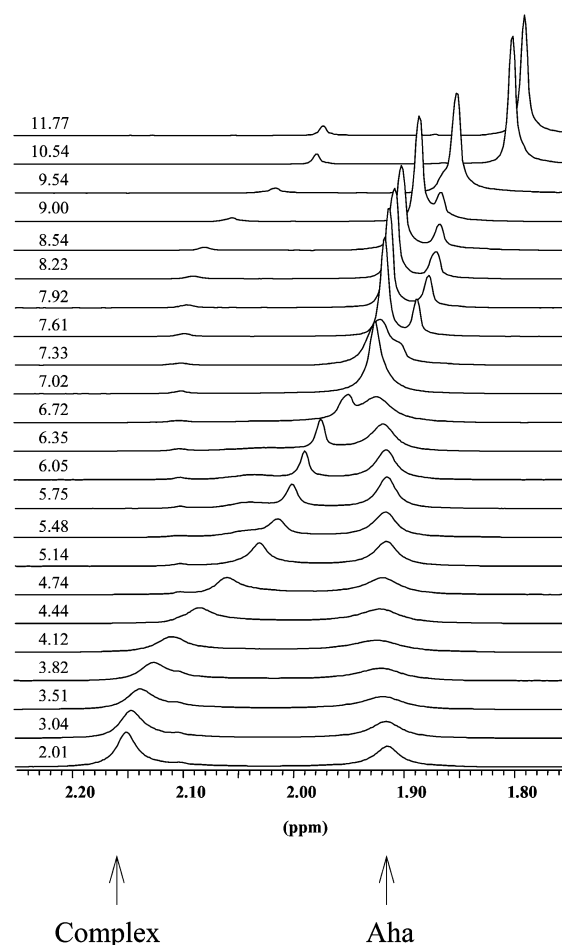


**Fig. 6**  $^1\text{H}$  NMR spectra of the Mo(vi)-Aha system at various pD values:  $c_{\text{Aha}} = 0.15$  M,  $c_{\text{Mo(vi)}} = 0.05$  M.

changes in the line-width of the signals as a function of pH refer to various inter- and intra-molecular exchange processes that occur in the system, e.g. broader signals refer to faster processes in the acidic region, while sharper ones indicate the formation of more inert species, while sharper ones indicate the formation of more inert species, while sharper ones indicate the formation of more inert species, while sharper ones indicate the formation of more inert species. Quantitative evaluation of the exchange processes, however, can not be made from the  $^1\text{H}$  NMR spectra.

A comparison of the  $^1\text{H}$  NMR results with those obtained from the  $^{17}\text{O}$  NMR spectra allows to draw the following conclusions: (i) the signal that appears at 2.151 ppm at pD = 2 and shifts down to ca. 1.85 ppm by pD = 9.5 belongs unambiguously to the three different  $\text{MoO}_2^{2+}$  core-containing species ( $[\text{MoO}_2\text{L}_2]$ ,  $[\text{MoO}_2\text{L}(\text{OH})_2]^-$  and  $[\text{MoO}_2(\text{LH}_{-1})]$ ); (ii) The pK values obtained by fitting the chemical shift vs. pD curve of that signal are the following:  $\text{p}K_1 = 4.55(5)$ ;  $\text{p}K_2 = 6.91(8)$ . These values are very close to those obtained by  $^{17}\text{O}$  NMR spectra (especially if we take into account the differences in the conditions applied and given in the Experimental section) and belong to processes (6) and (9). (iii) The relative intensities at pD = 2 are in accordance with the dominant formation of  $[\text{MoO}_2\text{L}_2]$ . (iv) The very broad signal appearing at pD = 5.48, 5.75 and 6.05 at 2.038, 2.038 and 2.035 ppm, respectively, belongs most probably to  $\text{MoO}_3$ -containing species.

Unfortunately, precipitation occurred in the acidic region in the Mo(vi)-Bha samples even in very dilute solutions. Dissolution of the precipitate allowed the measurements in the pD-range ca. 5–11 and some representative spectra registered for the free ligand and metal containing system are shown in Fig. 7(a) and (b). Although the spectra are quite complicated, there is no doubt that a multiplet signal belonging to molybdenum-Bha complexes (most probably  $\text{MoO}_2^{2+}$ -containing ones), exists almost in the whole measurable pD-range. This

**Table 2** A comparison of the results obtained by pH-metry and NMR methods for primary and secondary hydroxamic acid-containing systems

| System                | Model determined by  |  | Upper pH limit of Mo(vi)-ligand interactions |
|-----------------------|--|--|--|
|                       | pH-metry   | NMR  |  |
| Mo(vi)-DFB            | $[\text{MoO}_2(\text{H}_2\text{L})]^+$                                       | $[\text{MoO}_2(\text{H}_2\text{L})]^+$<br>$[\text{MoO}_3(\text{H}_3\text{L})]$   | ca. 8.5                                      |
| Mo(vi)-Aha/Mo(vi)-Bha | $[\text{MoO}_2\text{L}_2]$<br>$[\text{MoO}_3\text{L}(\text{H}_2\text{O})]^-$ | $[\text{MoO}_2\text{L}_2]$<br>$[\text{MoO}_2\text{L}(\text{OH})_2]^-$<br>$[\text{MoO}_3\text{L}(\text{H}_2\text{O})]^-$<br>$[\text{MoO}_2(\text{LH}_{-1})(\text{OH})_2]^{2-}$<br>$[\text{MoO}_3(\text{LH}_{-1})(\text{H}_2\text{O})]^{2-}$ | ca. 10.5                                     |
| Mo(vi)-MeAha          | $[\text{MoO}_2\text{L}_2]$<br>$[\text{MoO}_3\text{L}(\text{H}_2\text{O})]^-$ | $[\text{MoO}_2\text{L}_2]$<br>$[\text{MoO}_2\text{L}(\text{OH})_2]^-$<br>$[\text{MoO}_3\text{L}(\text{H}_2\text{O})]^-$  | ca. 8.5                                      |

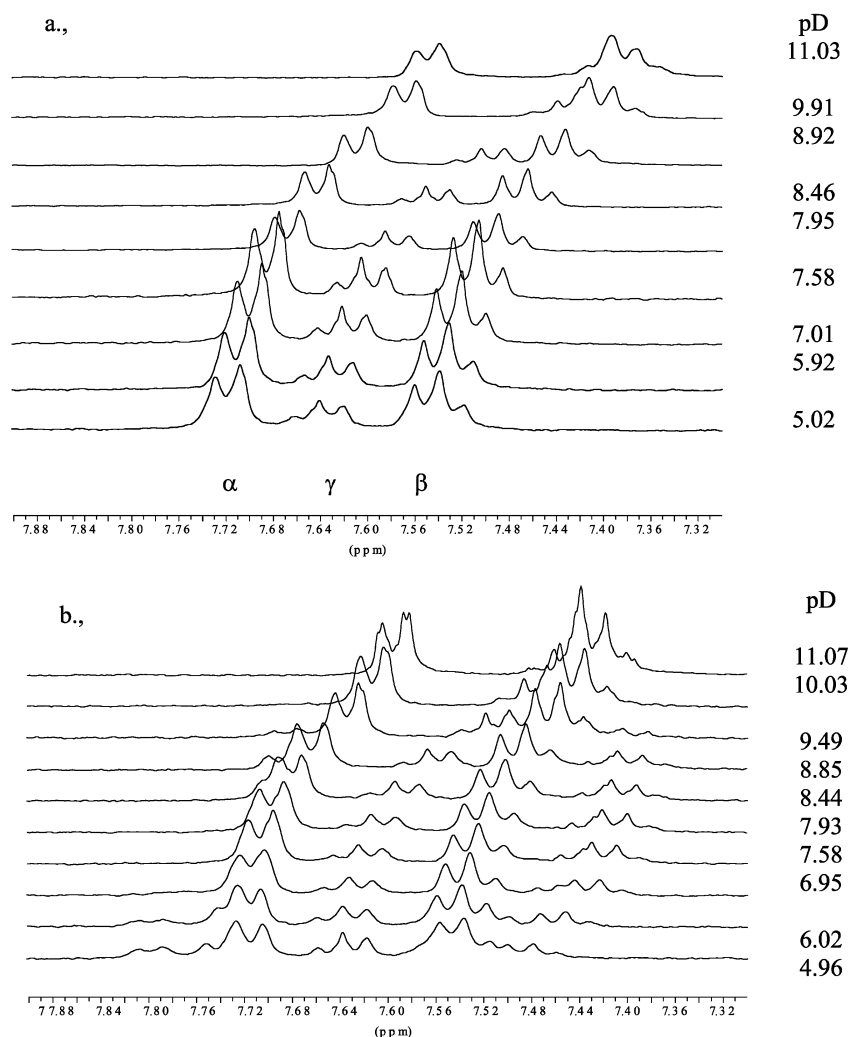


**Fig. 7**  $^1\text{H}$  NMR spectra of the H-Bha (a) and Mo(vi)-Bha (b) systems at various pD values:  $c_{\text{Bha}} = 0.014 \text{ M}$ ,  $c_{\text{Mo(vi)}} = 0.0052 \text{ M}$ .

signal shows a deprotonation process in the pD-range 5–8, for which a pK value of ca. 6.0–6.5 can be estimated.

All the  $^1\text{H}$  NMR results obtained in the pD-range 2–8 for the Mo(vi)-MeAha system supported the above conclusions. In the pD-range measured, in addition to the two singlets at 2.09 and 3.20 ppm belonging to the methyl protons next to the C and N atoms of the free ligand, respectively, two additional signals appear. One is at 2.20 ppm and the other at 3.47 ppm at pD = 2. The chemical shifts decrease by pD 5, down to 2.14 and 3.40 ppm, respectively. The pK value calculated from the spectra is 3.8(1) and most probably belongs to process (6). No further change occurs in the chemical shifts above pD ca. 5 at all and the signals of the complexes disappear by pD = 8. Consequently, the secondary ligand MeAha, which has no proton on its hydroxamate-N, is unable to form the very

stable hydroximato chelate and is displaced from the coordination sphere of Mo(vi) by hydrolysis at much lower pH (ca. 8) than for the primary hydroxamic acids Aha and Bha (above pH 10). These latter results give further support to the assumption that the deprotonation processes occurring in the Mo(vi)-Aha and Mo(vi)-Bha systems above pH 6 relate to the deprotonation of the NH protons of the coordinated hydroxamates.

### Conclusion

A comparison between the models obtained by pH-metric<sup>7</sup> and multinuclear NMR methods as well as between the different Mo(vi)-binding abilities of the various hydroxamic acids is made in Table 2.

As Table 2 shows, improved equilibrium models for all the studied systems, Mo(VI)-DFB, Mo(VI)-Aha, Mo(VI)-Bha and Mo(VI)-MeAha, were obtained by the use of the NMR methods. In addition to the very stable bis-hydroxamate, a small amount of mono-hydroxamate complex was also found in the Mo(VI)-DFB system. It was shown that both types of the possible mono-hydroxamate complexes,  $[\text{MoO}_2\text{L}(\text{OH})_2]^-$  and  $[\text{MoO}_3\text{L}(\text{H}_2\text{O})]^-$  are formed with monohydroxamic acids, in the slightly acidic and in the neutral pH region. Indication was found for the formation of a hydrogen bond between the hydroxamate-NH of the Aha and an oxo ligand of the metal ion under acidic conditions. Moreover, the NH proton of the coordinated monohydroxamic acids, Aha and Bha, dissociates above pH *ca.* 6 and the very stable hydroximate chelate is formed. As a result of this, the primary hydroxamic acids are able to chelate Mo(VI) up to pH 10 or somewhat above, but secondary type hydroxamic acids, which are unable to form a hydroximate chelate, are released by pH 8–8.5. This is the explanation of the interesting phenomenon as to why small primary monohydroxamic acids like Aha or Bha, are better chelators of Mo(VI) under basic conditions than the tri-hydroxamate-based siderophore, DFB.

### Acknowledgements

We are grateful for Hungarian Scientific Research Funds (OTKA projects T034674, T 38296 and TS 040685).

### References

1 A.-M. Albrecht-Gary and A. L. Crumbliss, in *Metal ions in*

- biological systems*, ed. H. Sigel and A. Sigel, Marcel Dekker, New York, 1998, vol. 35, p. 239.
- 2 K. N. Raymond, G. Müller and B. F. Matzanke, *Top. Curr. Chem.*, 1984, **123**, 49.
- 3 A.-K. Duhme, Z. Dauter, R. C. Hider and S. Pohl, *Inorg. Chem.*, 1996, **35**, 3059.
- 4 A.-K. Duhme, *J. Chem. Soc., Dalton Trans.*, 1997, 773.
- 5 P. Ghosh and A. Chakravorty, *Inorg. Chem.*, 1983, **22**, 1322.
- 6 D. A. Brown, H. Bogge, R. Coogan, D. Doocey, T. J. Kemp, A. Müller and B. Neumann, *Inorg. Chem.*, 1996, **35**, 1674.
- 7 E. Farkas, H. Csóka, G. Micera and A. Dessi, *J. Inorg. Biochem.*, 1997, **65**, 281.
- 8 E. Farkas, K. Megyeri, L. Somsák and L. Kovács, *J. Inorg. Biochem.*, 1998, **70**, 41.
- 9 E. Farkas, H. Csóka, G. Bell, D. A. Brown, L. P. Cuffe, N. J. Fitzpatrick, W. K. Glass, W. Errington and T. J. Kemp, *J. Chem. Soc., Dalton Trans.*, 1999, 2789.
- 10 E. Farkas and H. Csóka, *J. Inorg. Biochem.*, 2002, **89**, 219.
- 11 E. Farkas and A. V. Gerlei, in *Challenges for Coordination Chemistry in the New Century*, ed. M. Melnik and A. Sirota, Slovak Technical University Press, Bratislava, 2001, vol. 5, p. 365.
- 12 M. A. Freeman, F. A. Schultz and C. N. Reilly, *Inorg. Chem.*, 1982, **21**, 567.
- 13 K. F. Miller and A. D. Wentworth, *Inorg. Chem.*, 1979, **18**, 984.
- 14 O. W. Howarth and P. Kelly, *J. Chem. Soc. Dalton Trans.*, 1990, 81.
- 15 A. H. Blatt, *Org. Synth.*, 1943, **Collect. vol. II**, 67.
- 16 G. Gran, *Acta Chem. Scand.*, 1950, **4**, 559.
- 17 H. M. Irving, M. G. Miles and L. D. Pettit, *Anal. Chim. Acta.*, 1967, **38**, 475.
- 18 L. Zékány and I. Nagypál, in *Computational Methods for the Determination of Stability Constants*, ed. D. L. Leggett, Plenum Press, New York, 1985, p. 291.
- 19 E. Farkas, E. Kozma, M. Pethő, K. M. Herlihy and G. Micera, *Polyhedron*, 1998, **17**, 3331.